Synthesis and Characterization of Platinum-Gold Clusters Fused to Tetrahedral Copper Units. Crystal Structures of $[Pt(PPh_3)(AuPPh_3)_6(Cu_4Cl_3PPh_3)](NO_3)$ and $[Pt(PPh_3)(AuPPh_3)_6(Cu_4I_3)](NO_3)$

T. G. M. M. Kappen, P. P. J. Schlebos, J. J. Bour, W. P. Bosman, J. M. M. Smits, P. T. Beurskens, and J. J. Steggerda*

Contribution from the Department of Inorganic Chemistry and Crystallography, Faculty of Science, University of Nijmegen, Toernooiveld, 6525 ED Nijmegen, The Netherlands

Received August 12, 1994. Revised Manuscript Received March 28, 1995[⊗]

Abstract: Three new 11-metal-atom Pt-Au-Cu cluster compounds are reported: $[Pt(PPh_3)(AuPPh_3)_6(Cu_4Cl_3PPh_3)](NO_3)$ (**1**), $[Pt(PPh_3)(AuPPh_3)_6(Cu_4Br_3(PPh_3)_y)](NO_3)$ (**2**) ($y = 0$ or 1), and $[Pt(PPh_3)(AuPPh_3)_6(Cu_4I_3)](NO_3)$ (**3**). These clusters are obtained from the reaction of $[Pt(AuPPh_3)_8](NO_3)_2$ with $[PPh_3CuX]_4$ (in which X = Cl, Br, or I, respectively). Cluster **1** was characterized by elemental analysis, ICP analysis, FAB-MS, (variable-temperature) ^{31}P NMR and ^{31}P COSY spectroscopy, ^{195}Pt NMR spectroscopy, and IR spectroscopy. The crystal and molecular structure of **1** has been determined by a single-crystal X-ray analysis. The compound crystallizes as the NO_3^- salt in the triclinic space group $P\bar{1}$ with $Z = 2$, $a = 17.501(3)$ Å, $b = 21.152(6)$ Å, $c = 23.581(5)$ Å, $\alpha = 92.18(2)°$, $\beta = 94.61(1)°$, $\gamma = 109.69(2)°$, and $V = 8172$ Å^3. Mo Kα radiation was used. The residuals are $R = 0.068$ and $wR_2 = 0.162$ for 11040 observed reflections and 788 variables. Cluster **3** was characterized by ^{31}P NMR spectroscopy and FAB-MS; its solid-state structure was determined by means of a single-crystal X-ray analysis. This cluster compound crystallizes as the NO_3^- salt in the monoclinic space group $P2_1/c$, with $Z = 4$, $a = 17.871(4)$ Å, $b = 34.687(3)$ Å, $c = 23.357(2)$ Å, $\beta = 95.49(2)°$, and $V = 14412$ Å^3. Mo Kα radiation was used. The residuals are $R = 0.117$ and $wR_2 = 0.285$ for 2957 observed reflections and 340 variables. Both clusters, **1** and **3**, have a tetrahedral Cu_4 unit which is face (η^3) bonded to the (central) platinum atom, which is furthermore surrounded by six gold atoms. Short copper-gold and copper-platinum distances show that the copper atoms, although coagulated, are part of the metal cluster core. In cluster **1** an additional PPh_3 ligand is present on the Cu_4 unit as compared to **3**; in solution this copper-bonded phosphine of **1** is shown to dissociate reversibly. The cluster compound **2** was characterized by means of ^{31}P NMR spectroscopy, which indicates this cluster to be analogous to clusters **1** and **3**.

Introduction

The synthesis, characterization, and reactivity of mixed metal-gold clusters have been studied extensively over the last decade. These studies have shown the growing of metal clusters from 1 to 12 metal atoms in one-by-one metal atom addition steps. As molecular structures of many compounds could be determined by spectroscopic and single-crystal X-ray analysis, the structural accommodations necessary for the incorporation of another metal atom into the metal cluster could be seen in detail.

Of major interest with respect to cluster growth mechanisms is the electrophilic addition of M(I) species (M = Cu, Ag, Au):[1-3]

$$[Pt(AuPPh_3)_8]^{2+} + CuCl \rightarrow [Pt(CuCl)(AuPPh_3)_8]^{2+} \quad (1)$$

$$[Pt(AuPPh_3)_8]^{2+} + Ag^+ \rightarrow [Pt(Ag)(AuPPh_3)_8]^{3+} \quad (2)$$

$$[W(CO)_4(AuPPh_3)_5]^+ + AuPPh_3^+ \rightarrow [W(CO)_4(AuPPh_3)_6]^{2+} \quad (3)$$

Further additions of M(I) species to the toroidal clusters $[Pt(CuCl)(AuPPh_3)_8]^{2+}$ and $[Pt(Ag)(AuPPh_3)_8]^{3+}$ are blocked due to steric arguments, as the metal cluster is restricted to a toroidal geometry because of the presence of only 16 cluster valence electrons. After addition of 2 more electrons (to result in a total number of 18 cluster valence electrons) by nucleophilic addition of a base like PPh_3 or CO, the spherical geometry of the metal cluster allows further growth. So $PtCu_2Au_8$, $PtAg_2Au_8$ and $PtAg_3Au_6$ frames can only be obtained in spheroidal clusters.[4-6] It is noteworthy that the solid-state structures of these clusters are such that there are no direct Ag-Ag or Cu-Cu contacts: they are separately distributed among the peripheral metal atoms.

In contrast with these well-known one-by-one atom growth steps, very little is known about the growth of a metal frame by adherence of another multiatom metal cluster. In this paper we will show that cluster growth occurs by incorporation of a Cu_4 moiety, originating from the well-known $[PPh_3CuX]_4$

[⊗] Abstract published in *Advance ACS Abstracts*, August 1, 1995.

(1) Schoondergang, M. F. J.; Bour, J. J.; Schlebos, P. P. J.; Vermeer, A. W. P.; Bosman, W. P.; Smits, J. M. M.; Beurskens, P. T.; Steggerda, J. J. *Inorg. Chem.* **1991**, *30*, 4704.

(2) Kanters, R. P. F.; Schlebos, P. P. J.; Bour, J. J.; Bosman, W. P.; Smits, J. M. M.; Beurskens, P. T.; Steggerda, J. J. *Inorg. Chem.* **1990**, *29*, 324.

(3) Kappen, T. G. M. M.; van den Broek, A. C. M.; Schlebos, P. P. J.; Bour, J. J.; Bosman, W. P.; Smits, J. M. M.; Beurskens, P. T.; Steggerda, J. J. *Inorg. Chem.* **1992**, *31*, 4075.

(4) Kappen, T. G. M. M.; Schlebos, P. P. J.; Bour, J. J.; Bosman, W. P.; Smits, J. M. M.; Beurskens, P. T.; Steggerda, J. J. *Inorg. Chem.* Accepted for publication.

(5) Kappen, T. G. M. M.; Schlebos, P. P. J.; Bour, J. J.; Bosman, W. P.; Beurskens, G.; Smits, J. M. M.; Beurskens, P. T.; Steggerda, J. J. *Inorg. Chem.* Accepted for publication.

(6) Schoondergang, M. F. J. *New Developments in Platinum-Gold Cluster Chemistry;* University of Nijmegen: Nijmegen, The Netherlands, 1992.

0002-7863/95/1517-8327$09.00/0

compounds (in which X = Cl, Br, or I). In the newly formed compounds $[Pt(PPh_3)(AuPPh_3)_6(Cu_4Cl_3PPh_3)](NO_3)$ (**1**), $[Pt(PPh_3)(AuPPh_3)_6(Cu_4Br_3(PPh_3)_y)](NO_3)$ (**2**) ($y = 0$ or 1), and $[Pt(PPh_3)(AuPPh_3)_6(Cu_4I_3)](NO_3)$ (**3**) the 4 Cu atoms still hold their original tetrahedral adherence, but now integrated into a $PtAu_6Cu_4$ cluster frame. So two separate metal clusters merge into a new bigger entity.

Experimental Section

Measurements. Elemental C, H, and N analyses were carried out at the microanalytical department of the University of Nijmegen. ICP analyses giving Pt:Au:Cu ratios were carried out on a Plasma 200 ICP-AE spectrometer in DMSO solutions of the cluster compounds with $[Pt(CO)(CuCl)(AuPPh_3)_8](NO_3)_2$ (ref 1) and $[Pt(CO)(CuCl)_2(AuPPh_3)_7](NO_3)$ (ref 1) used for calibration. Fast atom bombardment mass spectroscopy (FAB-MS) was performed by the mass spectrometry service laboratory of the University of Minnesota on a VG Analytical Ltd. 7070E-HF mass spectrometer. The FAB-MS spectra were taken in a *m*-nitrobenzyl alcohol matrix and CsI was used as the mass-calibration standard; further experimental details are published elsewhere.[7]

$^{31}P\{^1H\}$ NMR spectra of CH_2Cl_2 solutions were recorded on a Bruker WM-200 spectrometer operating at 81.015 MHz and on a Bruker AM-500 spectrometer operating at 202.462 MHz with trimethyl phosphate (TMP) in CD_2Cl_2 as external reference. The variable-temperature $^{31}P\{^1H\}$ NMR spectra were recorded on the Bruker AM-500 spectrometer; the samples used in these experiments contained 100 mg of cluster compound in 1.5 mL of CD_2Cl_2.

Proton-decoupled ^{31}P COSY magnitude spectra[8] of CD_2Cl_2 solutions were recorded on the aforementioned Bruker AM-500 spectrometer at 298 K. The spectra were recorded with equal horizontal resolution in both directions: $[Pt(PPh_3)(AuPPh_3)_6(Cu_4Cl_3PPh_3)](NO_3)$ (**1**) was recorded with 2.0 Hz per point; $[Pt(PPh_3)(AuPPh_3)_6(Cu_4I_3)](NO_3)$ (**3**) was recorded with 3.7 Hz per point.

^{195}Pt NMR spectra were recorded at 43.02 MHz on a Bruker WM-200 spectrometer using CD_2Cl_2 solutions of the compounds; K_2PtCl_6 in D_2O was used as external reference. The infrared (IR) spectra were measured in CsI pellets on a Perkin-Elmer 1720-X Fourier transform infrared spectrometer in the range from 4000 to 220 cm^{-1}.

Preparations. $[PPh_3CuCl]_4$, $[PPh_3CuBr]_4$, and $[PPh_3CuI]_4$ were prepared according to literature methods.[9] This is also the case for $[Pt(AuPPh_3)_8](NO_3)_2$.[10] All solvents were of reagent grade and were used without further purification.

$[Pt(PPh_3)(AuPPh_3)_6(Cu_4Cl_3PPh_3)](NO_3)$ (1). A 100-mg (0.025 mmol) sample of $[Pt(AuPPh_3)_8](NO_3)_2$ was dissolved in 10 mL of acetone, and 27 mg (0.019 mmol) of $[PPh_3CuCl]_4$ was added to this brown solution. This mixture was stirred for 1 h after which it was allowed to stand for 2 days. Sometimes a red precipitate could be observed in minor amounts; therefore the brown solution was filtered. The brown filtrate was then concentrated to a volume of 2 mL by evaporation under reduced pressure upon which the orange-red cluster $[Pt(PPh_3)(AuPPh_3)_6(Cu_4Cl_3PPh_3)](NO_3)$ (**1**) precipitated slowly. After 1 day this precipitate was filtered off and washed with an acetone–diethyl ether (1:2) mixture and with diethyl ether (yield: 44 mg, 0.011 mmol; 60%, calculated for Cu). Orange-red single crystals of **1** suitable for X-ray analysis were obtained by slow diffusion of 1 mL of acetone, in which 8 mg of **1** was dissolved, into 4 mL of diethyl ether.

Anal. Calcd for $PtAu_6Cu_4P_8C_{144}H_{120}NO_3Cl_3$ (mol wt 3897.75): C, 44.37; H, 3.10; N, 0.36. Found: C, 43.84; H, 3.09; N, 0.36. ICP: Pt:Au:Cu = 1:5.9:4.0. IR: in addition to the bands due to PPh_3 only bands at 1346 cm^{-1} (uncoordinated NO_3) and at 311 cm^{-1} (CuCl stretching vibration) were present. ^{31}P NMR: singlet at δ 37.59 ppm with $^1J(P-^{195}Pt)$(doublet) = 2476 Hz; three closely spaced doublets at δ 52.26, 52.31, and 52.37 ppm all with $^4J(P-P)$(doublet) = 66 Hz and $^2J(P-^{195}Pt)$(doublet) = 358 Hz; three closely spaced doublets at δ 58.74, 58.80, and 58.88 ppm all with $^4J(P-P)$(doublet) = 66 Hz and $^2J(P-^{195}Pt)$(doublet) = 450 Hz. In cases where the horizontal resolution was not high enough, the closely spaced doublets could not be detected separately and two broader doublets were observed at δ 52.3 and 58.8 ppm with corresponding couplings as afore-mentioned; the intensities of both doublets were three times that of the singlet at δ 37.59 ppm. The variable-temperature ^{31}P NMR spectra (273–233 K) revealed the presence of the copper-bonded PPh_3 group at δ −5.0 ppm (singlet) (see Results and Discussion).

$^{195}Pt\{^1H\}$ NMR: δ −5761 ppm with a complex splitting pattern that can be perfectly simulated with $^1J(Pt-P)$(doublet) = 2476 Hz, $^2J(Pt-P)$(quartet) = 358 Hz, and $^2J(Pt-P)$(quartet) = 450 Hz, in accordance with the ^{31}P NMR data. The appearance of the ^{195}Pt NMR spectrum without proton decoupling was exactly the same, indicating the absence of $J(Pt-H)$ for **1**.

$[Pt(PPh_3)(AuPPh_3)_6(Cu_4Br_3(PPh_3)_y)](NO_3)$ (2) ($y = 0$ or 1). A 100-mg (0.025-mmol) sample of $[Pt(AuPPh_3)_8](NO_3)_2$ was dissolved in 10 mL of acetone, and 31 mg (0.019 mmol) of $[PPh_3CuBr]_4$ was added. This brown mixture was stirred for 1 h after which it was allowed to stand. After 1 day the reaction mixture had turned red. The solution was then evaporated to dryness and a ^{31}P NMR spectrum of this sample showed that **2** had been formed (yield: about 50%, based on the relative intensities in the ^{31}P NMR spectrum of this crude mixture). Several attempts to purify this mixture were not successful.

Compound **2** has not been analyzed by elemental analysis because the product could not be obtained as pure material. However, comparison of the ^{31}P NMR data of compounds **1**, **2**, and **3** (see Results and Discussion), together with a comparison of the synthesis procedures of these three compounds, indicates **2** to be closely related to compounds **1** and **3**. Therefore, **2** is most probably formulated as $[Pt(PPh_3)(AuPPh_3)_6(Cu_4Br_3(PPh_3)_y)](NO_3)$ ($y = 0$ or 1). ^{31}P NMR: singlet at δ 38.4 ppm (relative intensity 1) with $^1J(P-^{195}Pt)$(doublet) = 2479 Hz; doublet at δ 51.6 ppm (relative intensity 3) with $^4J(P-P)$(doublet) = 68 Hz and $^2J(P-^{195}Pt)$(doublet) = 344 Hz; doublet at δ 58.2 ppm (relative intensity 3) with $^4J(P-P)$(doublet) = 68 Hz and $^2J(P-^{195}Pt)$(doublet) = 460 Hz. Shoulders on the doublet peaks indicate that these doublets are a result of closely spaced signals as seen for compound **1**.

$[Pt(PPh_3)(AuPPh_3)_6(Cu_4I_3)](NO_3)$ (3). To a solution of 100 mg (0.025 mmol) of $[Pt(AuPPh_3)_8](NO_3)_2$ in 10 mL of acetone was added 45.4 mg (0.025 mmol) of $[PPh_3CuI]_4$. The color changed from brown to orange-red within 5 min and the mixture was stirred for 48 h. The solution was then filtered to remove possible minor solid contaminations. The orange-red filtrate was evaporated to dryness under reduced pressure to yield an orange-red solid in quantitative amounts. Red crystals, all of the same morphology, were obtained by slow diffusion of a dichloromethane solution of this orange-red solid into petroleum ether 40/60. One of these crystals was used for a single-crystal X-ray analysis, which revealed the molecular structure of **3**. However, solution ^{31}P NMR data of bulk material of these crystals (see below) showed the presence of a second product in constant ratio to **3**. Various attempts to separate these two products were not successful: the ^{31}P NMR spectrum always showed the unchanged ratio of **3** to unknown product as approximately 1:5 (see Results and Discussion).

Compound **3** has not been analyzed by elemental analysis because the product could not be obtained as pure material. Its solid-state structure has been determined by means of a single-crystal X-ray analysis (see below). FAB-MS also confirmed the presence of **3** in the red crystals (see Results and Discussion). ^{31}P NMR: singlet at δ 36.2 ppm (relative intensity 1) with $^1J(P-^{195}Pt)$(doublet) = 2458 Hz; doublet at δ 50.7 ppm (relative intensity 3) with $^4J(P-P)$(doublet) = 66 Hz and $^2J(P-^{195}Pt)$(doublet) = 368 Hz; doublet at δ 57.0 ppm (relative intensity 3) with $^4J(P-P)$(doublet) = 66 Hz and $^2J(P-^{195}Pt)$(doublet) = 445 Hz. Shoulders on the doublet peaks indicate that these doublets are a result of closely spaced, overlapping signals as seen for compound **1**.

The unknown product which was always seen in the ^{31}P NMR spectra together with **3** has the following data: singlet at δ 38.4 ppm with $^1J(P-^{195}Pt)$(doublet) = 2812 Hz; doublet at δ 45.4 ppm with $^4J(P-P)$(doublet) = 65 Hz and $^2J(P-^{195}Pt)$(doublet) = 314 Hz; singlet at δ

(7) Boyle, P. D.; Johnson, B. J.; Alexander, B. D.; Casalnuovo, J. A.; Gannon, P. R.; Johnson, S. M.; Larka, E. A.; Mueting, A. M.; Pignolet, L. H. *Inorg. Chem.* **1987**, *26*, 1346.

(8) Aue, W. P.; Bartholdi, E.; Ernst, R. R. *J. Chem. Phys.* **1976**, *64*, 2229.

(9) Costa, G.; Reisenhofer, E.; Stefani, L. *J. Inorg. Nucl. Chem.* **1965**, *27*, 2581.

(10) Bour, J. J.; Kanters, R. P. F.; Schlebos, P. P. J.; Steggerda, J. J. *Recl. Trav. Chim. Pays-Bas* **1988**, *107*, 211.

Table 1. Crystal Data for $[Pt(PPh_3)(AuPPh_3)_6(Cu_4Cl_3PPh_3)](NO_3)$ (**1**) and $[Pt(PPh_3)(AuPPh_3)_6(Cu_4I_3)](NO_3)$ (**3**)

compound	1	3
chemical formula[a]	$C_{144}H_{120}NO_3Au_6Cl_3Cu_4P_8Pt$	$C_{126}H_{105}NO_3Au_6Cu_4I_3P_7Pt$
formula weight	3897.8	3909.8
a/Å	17.501(3)	17.871(4)
b/Å	21.152(6)	34.687(3)
c/Å	23.581(5)	23.357(2)
α/deg	92.18(2)	90
β/deg	94.61(1)	95.49(2)
γ/deg	109.69(2)	90
V/Å^3	8172	14412
Z	2	4
space group	$P\bar{1}$(No. 2)	$P2_1/c$(No. 14)
T/°C	20	20
λ/Å	0.7107	0.7107
ϱ_{calc}/g·cm^{-3}	not calculated because of uncertainty in solvent content	
μ(MoKα)/cm^{-1}[a]	68.88	83.75
R[b] [$I > 2\sigma(I)$]	0.068	0.117
wR_2[c] [$I > 2\sigma(I)$]	0.162	0.285

[a] Solvent molecules not included. [b] $R = \sum||F_o| - |F_c||/\sum|F_o|$. [c] $wR_2 = [\sum w(F_o^2 - F_c^2)^2/\sum w(F_o^2)^2]^{1/2}$.

51.8 ppm with $^2J(P-^{195}Pt)$(doublet) = 388 Hz; doublet at δ 58.1 ppm with $^4J(P-P)$(doublet) = 65 Hz and $^2J(P-^{195}Pt)$(doublet) = 464 Hz. It was shown by ^{31}P COSY NMR spectroscopy that all these resonances belonged to the unknown product and that they were not coupled to that of **3** (see Results and Discussion).

Structure Determination of $[Pt(PPh_3)(AuPPh_3)_6(Cu_4Cl_3PPh_3)](NO_3)$ (1) and $[Pt(PPh_3)(AuPPh_3)_6(Cu_4I_3)](NO_3)$ (3). Collection and Reduction of Crystallographic Data. Since single crystals decomposed very quickly upon removal from the solvent mixture, a crystal of **1** was mounted in a capillary together with a mixture of acetone and diethyl ether and a crystal of **3** was mounted in a capillary together with a mixture of dichloromethane and petroleum ether 40/60. X-ray data were measured on a Nonius CAD4 diffractometer. For **3** 14250 reflections (h: 0 to 17; k: 0 to 33; l: −22 to 22; $1 \le \theta \le 20°$) were measured with a maximum scan time of 20 s/reflection. This set contained only 2150 observed ($I > 3\sigma(I)$) reflections. All the reflections with a standard deviation of 1.5−4 $\sigma(I)$ were remeasured with a maximum scan time of 180 s/reflection. This resulted in 2306 reflections of which 1290 were "observed". These two sets for **3** were merged. Other standard experimental details for **1** and **3** are given elsewhere.[11] Crystal data for **1** and **3** are given in Table 1.

Solution and Refinement of the Structures. $[Pt(PPh_3)(AuPPh_3)_6(Cu_4Cl_3PPh_3)](NO_3)$ (1). The positions of the metal atoms and ca. 80% of the phenyl carbon atoms were found from an automatic orientation and translation search (ORIENT,[12] TRACOR[13]) with a Au_6Cu_4 fragment of **3** as a search model, followed by a phase refinement procedure to expand the fragment (DIRDIF[14]). The other phenyl rings and one NO_3^- were positioned from difference Fourier maps. The hydrogen atoms on the phenyl rings were placed at calculated positions (C−H = 0.93 Å). Of the unknown amount of solvent molecules none could be detected. An additional empirical absorption correction based on $F_o - |F_c|$ was applied using DIFABS[15] on the original unmerged F_o values.

The structure was refined by full-matrix least-squares on F_o^2 values using SHELXL[16] with anisotropic parameters for the metal, phosphorus, and chlorine atoms and isotropic parameters for the carbon atoms. The NO_3^- ion and the phenyl rings were refined with constrained idealized geometry. The refinement converged at $R = 0.068$. The function minimized was $\sum w(F_o^2 - F_c^2)^2$ with $w = 1/[\sigma^2(F_o^2) + (0.057F_c^2)^2]$. A maximum residual density of 1.4 e/Å^3 was found near metal atoms.

The volume between the cluster molecules is 2280 Å^3 (28 vol %) (PLATON[17]); this volume is filled with unidentified solvent molecules.

Selected bond distances and bond angles are given in Table 2. The molecular structure of **1** is given in Figure 1.[18]

$[Pt(PPh_3)(AuPPh_3)_6(Cu_4I_3)](NO_3)$ (3). The positions of the metal atoms were found from automatic Patterson interpretation (PATTY[19]) followed by a phase refinement procedure to expand the fragment (DIRDIF[14]). The phenyl rings were positioned from successive difference Fourier maps. At this stage the NO_3^- ion has not been located, and of the unknown amount of solvent molecules none could be detected.

The phenyl rings were refined with constrained idealized geometry, with the hydrogen atoms placed at calculated positions (C−H = 0.93 Å). An additional empirical absorption correction based on $F_o - |F_c|$ was applied using DIFABS[15] on the original unmerged F_o values. The structure was refined by full-matrix least-squares on F_o^2 values using SHELXL[16] with anisotropic parameters for the metal, phosphorus, and iodine atoms and isotropic parameters for the carbon atoms. The refinement converged at $R = 0.117$. The function minimized was $\sum w(F_o^2 - F_c^2)^2$ with $w = 1/[\sigma^2(F_o^2) + (0.114F_c^2)^2]$. The relatively large R value is caused by the disorder in the NO_3^- ions and the solvent molecules. A maximum residual density of 2.2 e/Å^3 was found near metal atoms.

Table 2. Selected Bond Lengths (Å) and Bond Angles (deg) for $[Pt(PPh_3)(AuPPh_3)_6(Cu_4Cl_3PPh_3)](NO_3)$ (**1**)

Pt(1)−Au(2)	2.740(2)	Au(4)−Cu(4)	2.692(3)
Pt(1)−Au(3)	2.754(2)	Au(5)−Cu(2)	2.702(3)
Pt(1)−Au(4)	2.734(2)	Au(6)−Cu(3)	2.815(3)
Pt(1)−Au(5)	2.716(2)	Au(7)−Cu(4)	2.718(3)
Pt(1)−Au(6)	2.716(2)	Au(2)−P(2)	2.304(8)
Pt(1)−Au(7)	2.721(2)	Au(3)−P(3)	2.301(8)
Pt(1)−Cu(2)	2.632(3)	Au(4)−P(4)	2.297(8)
Pt(1)−Cu(3)	2.608(3)	Au(5)−P(5)	2.329(8)
Pt(1)−Cu(4)	2.617(3)	Au(6)−P(6)	2.319(8)
Pt(1)−P(1)	2.338(7)	Au(7)−P(7)	2.309(8)
Au(2)−Au(5)	2.849(2)	Cu(2)−Cu(3)	2.562(5)
Au(2)−Au(6)	2.881(2)	Cu(2)−Cu(4)	2.577(5)
Au(3)−Au(6)	2.814(2)	Cu(3)−Cu(4)	2.563(5)
Au(3)−Au(7)	2.880(2)	Cu(1)−P(8)	2.223(8)
Au(4)−Au(5)	2.916(2)	Cu(1)−Cl(1)	2.415(9)
Au(4)−Au(7)	2.891(2)	Cu(1)−Cl(2)	2.378(9)
Au(2)−Cu(2)	2.768(4)	Cu(1)−Cl(3)	2.427(9)
Au(2)−Cu(3)	2.632(3)	Cu(2)−Cl(2)	2.167(8)
Au(3)−Cu(3)	2.675(4)	Cu(3)−Cl(1)	2.189(7)
Au(3)−Cu(4)	2.671(3)	Cu(4)−Cl(3)	2.181(8)
Au(4)−Cu(2)	2.658(3)		
Au(2)−Pt(1)−Au(6)	62.94(4)	Cu(2)−Pt(1)−Cu(3)	58.55(11)
Au(2)−Pt(1)−Au(7)	63.74(4)	Cu(2)−Pt(1)−Cu(4)	58.81(10)
Au(3)−Pt(1)−Au(6)	61.92(4)	Cu(3)−Pt(1)−Cu(4)	58.75(10)
Au(3)−Pt(1)−Au(7)	63.49(4)	Pt(1)−Au(2)−P(2)	175.0(2)
Au(4)−Pt(1)−Au(5)	64.68(4)	Pt(1)−Au(3)−P(3)	179.2(2)
Au(4)−Pt(1)−Au(7)	64.01(4)	Pt(1)−Au(4)−P(4)	175.3(2)
Au(2)−Pt(1)−Cu(2)	62.00(8)	Pt(1)−Au(5)−P(5)	171.6(2)
Au(2)−Pt(1)−Cu(3)	58.90(8)	Pt(1)−Au(6)−P(6)	167.0(2)
Au(3)−Pt(1)−Cu(3)	59.79(8)	Pt(1)−Au(7)−P(7)	171.2(3)
Au(3)−Pt(1)−Cu(4)	59.58(8)	Pt(1)−Cu(2)−Cl(2)	164.4(3)
Au(4)−Pt(1)−Cu(2)	59.35(8)	Pt(1)−Cu(3)−Cl(1)	161.3(3)
Au(4)−Pt(1)−Cu(4)	60.36(8)	Pt(1)−Cu(4)−Cl(3)	165.3(3)
Au(5)−Pt(1)−Cu(2)	60.67(8)	Cu(1)−Cl(1)−Cu(3)	93.4(3)
Au(6)−Pt(1)−Cu(3)	63.81(8)	Cu(1)−Cl(2)−Cu(2)	90.6(3)
Au(7)−Pt(1)−Cu(4)	61.18(8)	Cu(1)−Cl(3)−Cu(4)	90.5(3)

(11) Smits, J. M. M.; Behm, H.; Bosman, W. P.; Beurskens, P. T. *J. Crystallogr. Spectrosc. Res.* **1988**, *18*, 447.
(12) Beurskens, P. T.; Beurskens, G.; Strumpel, M.; Nordman, C. E. *Patterson and Pattersons*; Glusker, J. P., Patterson, B. K., Rossi, M., Eds.; Clarendon Press: Oxford, 1987; p 356.
(13) Beurskens, P. T.; Gould, R. O.; Bruins Slot, H. J.; Bosman, W. P. *Z. Kristallogr.* **1987**, *179*, 127.
(14) Beurskens, P. T.; Admiraal, G.; Beurskens, G.; Bosman, W. P.; Garcia-Granda, S.; Gould, R. O.; Smits, J. M. M.; Smykalla, C. *The DIRDIF Program System, Technical Report of the Crystallography Laboratory*; University of Nijmegen: Nijmegen,The Netherlands, 1992.
(15) Walker, N.; Stuart, D. *Acta Crystallogr.* **1983**, *A39*, 158.
(16) Sheldrick, G. M. *SHELXL-92, Program for the Refinement of Crystal Structures*; University of Goettingen: Goettingen, Germany, 1992.
(17) Spek, A. L. *PLATON-93*; Bijvoet Center for Biomolecular Research, University of Utrecht: Utrecht, The Netherlands, 1993.
(18) Johnson, C. K. *ORTEP-II, Report on ORNL-5138*; Oak Ridge National Laboratory: Oak Ridge, TN, 1976.
(19) Admiraal, G.; Behm, H.; Smykalla, C.; Beurskens, P. T. *Z. Kristallogr.* **1992**, *Suppl. 6*, 522.

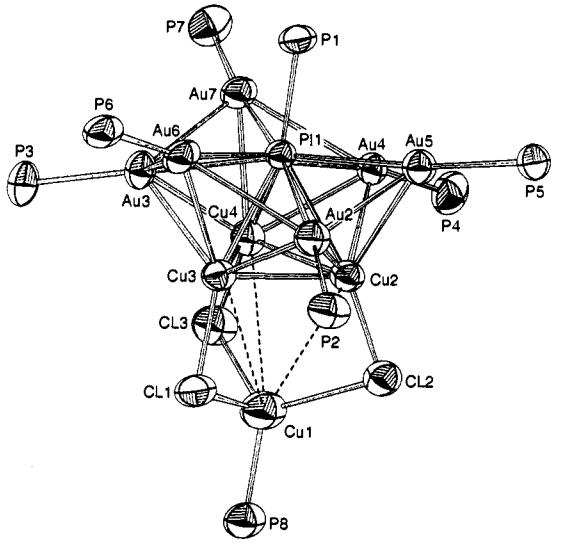

Figure 1. X-ray structure of $[Pt(PPh_3)(AuPPh_3)_6(Cu_4Cl_3PPh_3)](NO_3)$ (**1**) with atom labeling for Pt, Au, Cu, P, and Cl. Phenyl rings and the NO_3^- ion have been omitted for clarity. Thermal ellipsoids are at 50% probability.

The volume between the cluster molecules is 4065 Å^3 (28 vol %) (PLATON[17]); this volume is filled with unidentified solvent molecules and with four NO_3^- ions per cell.

Selected bond distances and bond angles are given in Table 3. The molecular structure of **3** is given in Figure 6.[18]

Results and Discussion

Synthesis, Characterization, and Crystal Structure of $[Pt(PPh_3)(AuPPh_3)_6(Cu_4Cl_3PPh_3)](NO_3)$ (1). The 11-metal-atom cluster compound $[Pt(PPh_3)(AuPPh_3)_6(Cu_4Cl_3PPh_3)](NO_3)$ (**1**) is obtained from the reaction of $[Pt(AuPPh_3)_8](NO_3)_2$ with $[PPh_3CuCl]_4$ in acetone in 60% yield. This orange-red compound was characterized by means of elemental analysis, ICP analysis, FAB-MS, IR, ^{31}P NMR (including variable-temperature ^{31}P NMR and ^{31}P COSY experiments), and ^{195}Pt NMR spectroscopy. The solid-state structure of **1** was obtained from a single-crystal X-ray analysis.

Crystal Structure. The X-ray structure analysis of the solid, together with the ^{31}P NMR data (vide infra), shows that **1** has a central platinum atom that is connected to a PPh_3 ligand, six $AuPPh_3$ units and a $Cu_4Cl_3PPh_3$ unit (Figure 1). The six $AuPPh_3$ units, are divided over two layers which are arranged in a staggered way. The $Cu_4Cl_3PPh_3$ unit consists of a distorted Cu_4 tetrahedron which is η^3 (face) bonded to the platinum atom; short copper–gold, copper–platinum, and copper–copper distances show that this unit is part of the cluster core. Cu(1) is bonded to a phosphine. Three μ_2-Cl ligands are bridging the copper atoms. So **1** can be seen as a $PtAu_6$ cluster unit which is fused to a tetrahedral Cu_4 cluster unit; fusion of smaller subunits is a helpful view to understanding cluster topology.[20,21] The Cu–Cu distances between Cu(2), Cu(3), and Cu(4) (2.562–2.577 Å) are short, compared to Cu–Cu distances known from the literature;[22–33] they are substantially shorter than the Cu–Cu distances to the phosphine-bonded Cu(1) (3.236–3.352 Å). These latter distances are comparable to Cu–Cu distances in e.g. $[PPh_3CuCl]_4$.[23] The Cu–Cu distances, together with the Cu–Cl distances (Table 2), are such that Cu(1) can be viewed as pulled away from the Cu(2)–Cu(3)–Cu(4) triangle; this may be due to the coordination of the phosphine ligand to Cu(1). Support for this can be obtained from the related solid-state structure of **3** (vide infra).

The Pt–Cu distances and the Au–Cu distances to the copper atoms Cu(2), Cu(3), and Cu(4), together with the Pt–Au distances and the Au–Au distances, are all in the range normally observed;[1,2,34–39] the Pt–Cu and Au–Cu bond lengths are smaller than the Pt–Au and Au–Au bond lengths, respectively (Table 2).

Table 3. Selected Bond Lengths (Å) and Bond Angles (deg) for $[Pt(PPh_3)(AuPPh_3)_6(Cu_4I_3)](NO_3)$ (**3**)

Pt(1)–Au(2)	2.765(6)	Au(4)–Cu(4)	2.758(10)
Pt(1)–Au(3)	2.783(5)	Au(5)–Cu(2)	2.760(9)
Pt(1)–Au(4)	2.751(6)	Au(6)–Cu(3)	2.854(9)
Pt(1)–Au(5)	2.720(5)	Au(7)–Cu(4)	2.746(10)
Pt(1)–Au(6)	2.703(6)	Au(2)–P(2)	2.30(2)
Pt(1)–Au(7)	2.722(6)	Au(3)–P(3)	2.31(2)
Pt(1)–Cu(4)	2.688(10)	Au(4)–P(4)	2.32(2)
Pt(1)–Cu(2)	2.691(9)	Au(5)–P(5)	2.32(2)
Pt(1)–Cu(3)	2.712(8)	Au(6)–P(6)	2.30(2)
Pt(1)–P(1)	2.34(2)	Au(7)–P(7)	2.30(2)
Au(2)–Au(5)	2.847(6)	Cu(1)–Cu(2)	2.69(2)
Au(2)–Au(6)	2.900(6)	Cu(1)–Cu(3)	2.70(2)
Au(3)–Au(6)	2.861(6)	Cu(1)–Cu(4)	2.69(2)
Au(3)–Au(7)	2.908(6)	Cu(2)–Cu(3)	2.703(12)
Au(4)–Au(5)	2.952(6)	Cu(2)–Cu(4)	2.702(13)
Au(4)–Au(7)	2.882(6)	Cu(3)–Cu(4)	2.720(14)
Au(2)–Cu(2)	2.828(10)	I(1)–Cu(1)	2.63(2)
Au(2)–Cu(3)	2.711(8)	I(1)–Cu(2)	2.508(12)
Au(3)–Cu(3)	2.754(8)	I(2)–Cu(1)	2.61(2)
Au(3)–Cu(4)	2.695(10)	I(2)–Cu(3)	2.526(11)
Au(4)–Cu(2)	2.709(9)	I(3)–Cu(4)	2.484(12)
Au(2)–Pt(1)–Au(5)	62.5(2)	Pt(1)–Au(5)–P(5)	172.3(7)
Au(2)–Pt(1)–Au(6)	64.0(2)	Pt(1)–Au(6)–P(6)	171.2(7)
Au(3)–Pt(1)–Au(6)	62.8(2)	Pt(1)–Au(7)–P(7)	170.1(6)
Au(3)–Pt(1)–Au(7)	63.8(2)	I(1)–Cu(2)–Pt(1)	166.9(4)
Au(4)–Pt(1)–Au(5)	65.3(2)	I(2)–Cu(3)–Pt(1)	167.0(4)
Au(4)–Pt(1)–Au(7)	63.5(2)	I(3)–Cu(4)–Pt(1)	165.5(5)
Au(2)–Pt(1)–Cu(2)	62.4(2)	Cu(2)–Cu(1)–Cu(3)	60.2(4)
Au(2)–Pt(1)–Cu(3)	59.3(2)	Cu(2)–Cu(1)–Cu(4)	60.3(4)
Au(3)–Pt(1)–Cu(4)	59.0(2)	Cu(3)–Cu(1)–Cu(4)	60.6(4)
Au(3)–Pt(1)–Cu(3)	60.2(2)	Cu(1)–Cu(2)–Cu(3)	59.8(3)
Au(4)–Pt(1)–Cu(2)	59.7(2)	Cu(1)–Cu(2)–Cu(4)	59.8(4)
Au(4)–Pt(1)–Cu(4)	60.9(2)	Cu(3)–Cu(2)–Cu(4)	60.4(3)
Au(5)–Pt(1)–Cu(2)	61.3(2)	Cu(1)–Cu(3)–Cu(2)	59.8(4)
Au(6)–Pt(1)–Cu(3)	63.6(2)	Cu(1)–Cu(3)–Cu(4)	59.5(4)
Au(7)–Pt(1)–Cu(4)	61.0(2)	Cu(2)–Cu(3)–Cu(4)	59.8(3)
Cu(2)–Pt(1)–Cu(3)	60.0(3)	Cu(1)–Cu(4)–Cu(2)	59.9(4)
Cu(2)–Pt(1)–Cu(4)	60.3(3)	Cu(1)–Cu(4)–Cu(3)	59.8(5)
Cu(3)–Pt(1)–Cu(4)	60.5(3)	Cu(2)–Cu(4)–Cu(3)	59.8(3)
Pt(1)–Au(2)–P(2)	176.5(7)	Cu(2)–I(1)–Cu(1)	63.1(4)
Pt(1)–Au(3)–P(3)	174.3(6)	Cu(3)–I(2)–Cu(1)	63.4(4)
Pt(1)–Au(4)–P(4)	177.7(6)	Cu(4)–I(3)–Cu(1)	64.4(4)

(20) King, R. B. *Inorg. Chim. Acta*, **1993**, *212*, 57.
(21) Teo, B. K.; Shi, X.; Zhang, H. *Inorg. Chem.* **1993**, *32*, 3987 and references cited therein.
(22) Draper, M. D.; Hattersley, A. D.; Housecroft, C. E.; Rheingold *J. Chem. Soc., Chem. Commun.* **1992**, 1365.
(23) Churchill, M. R.; Kalra, K. L *Inorg. Chem.* **1974**, *13*, 1065.
(24) Barron, P. F.; Dyason, J. C.; Engelhardt, L. M.; Healy, P. C.; White, A. H. *Inorg. Chem.* **1984**, *23*, 3766.
(25) Dyason, J. C.; Healy, P. C.; Engelhardt, L. M.; Pakawatchai, C.; Patrick, V. A.; Raston, C. L.; White, A. H. *J. Chem. Soc., Dalton Trans.* **1985**, 831.
(26) Coucouvanis, D.; Kanodia, S.; Swenson, D.; Chen, S. J.; Stüdemann, T.; Baenziger, N. C.; Pedelty, R.; Chu, M. *J. Am. Chem. Soc.* **1993**, *115*, 11271.
(27) Churchill, M. R.; Youngs, W. J. *Inorg. Chem.* **1979**, *18*, 1133.
(28) Filippo, J. S.; Zyontz, L. E.; Potenza, J. *Inorg. Chem.* **1975**, *14*, 1667.
(29) Churchill, M. R.; Kalra, K. L *Inorg. Chem.* **1974**, *13*, 1899.
(30) Raston, C. L.; White, A. H. *J. Chem. Soc., Dalton Trans.* **1976**, 2153.
(31) Schramm, V. *Inorg. Chem.*, **1978**, *17*, 714.
(32) Naldini, L.; Demartin, F.; Manassero, M.; Sansoni, M.; Rasso, G.; Zoroddu, M. A. *J. Organomet. Chem.* **1985**, *279*, C24.
(33) Eichhöfer, A.; Fenske, D.; Holstein, W. *Angew. Chem., Int. Ed. Engl.* **1993**, *32*, 242.
(34) Kanters, R. P. F.; Schlebos, P. P. J.; Bour, J. J.; Bosman, W. P.; Behm, H. J.; Steggerda, J. J. *Inorg. Chem.* **1988**, *27*, 4034.

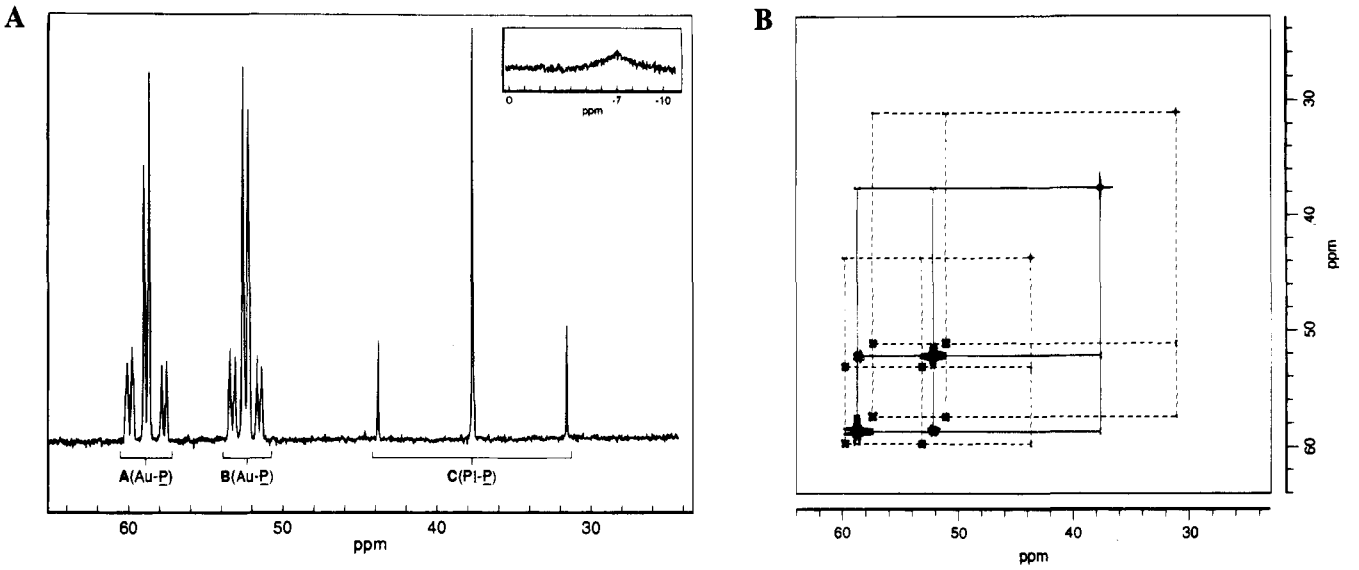

Figure 2. (A) ^{31}P NMR spectrum (202.462 MHz) at 298 K of $[Pt(PPh_3)(AuPPh_3)_6(Cu_4Cl_3PPh_3)](NO_3)$ (**1**). (B) ^{31}P COSY NMR spectrum (202.462 MHz) at 298 K of $[Pt(PPh_3)(AuPPh_3)_6(Cu_4Cl_3PPh_3)](NO_3)$ (**1**).

The $AuPPh_3$ groups, the platinum-bonded phosphine, and the Cu_4 unit surround the (central) platinum atom in a (quasi-)-spheroidal symmetry, as indicated by the topological parameters S and P,[40] which are 0.97 and 0.99, respectively. This spheroidal surrounding of the platinum atom is in accordance with the $(S^{\sigma})^2(P^{\sigma})^6$ electron configuration (18 electrons) of **1** (the neutral fictitious $Cu_4Cl_3PPh_3$ entity is taken to donate one electron).

The presence of Cu–Cl bonds as derived from the X-ray structure analysis has also been evidenced by IR spectroscopy: the Cu–Cl stretching vibration of **1** is observed at 311 cm^{-1}. The solid-state structure as reported is in full agreement with the physical bulk data including elemental C, H, and N analysis and ICP analysis (see Experimental Section).

NMR Spectroscopy. The ^{31}P NMR spectrum of **1** at room temperature (Figure 2A) shows resonances that can be assigned to the different phosphine sites as observed in the crystal structure of this cluster. This indicates that **1** shows no intramolecular fluxionality at room temperature and in contrast to many of the known mixed metal–gold cluster compounds whose ^{31}P NMR spectra show fluxional behavior at room temperature,[1-5,34,41,42] which for some clusters can be frozen by lowering the temperature.[3,43]

For **1** a singlet at δ 37.59 ppm is observed that belongs to the platinum-bonded phosphine ligand (P(1)) as evidenced by the value of the $J(P-^{195}Pt)$. Small spin–spin couplings between the platinum-bonded phosphine and the gold-bonded phosphines, although not detectable from the one-dimensional ^{31}P NMR spectrum, are observed from the ^{31}P COSY spectrum of **1** (Figure 2B; crosspeaks between sites A and C, and between sites B and C).

The six gold-bonded phosphines are all individually observed. Three sites are observed as three closely separated doublets near δ 52.3 ppm (sites B in Figure 2A) and three other closely separated doublets are found near δ 58.8 ppm (sites A in Figure 2A). Sites A and B correspond to the two $AuPPh_3$ triangles Au(2)–Au(3)–Au(4) and Au(5)–Au(6)–Au(7), respectively. The doublet nature of these sites is due to a $^4J(P-P)$ coupling of one phosphine site of the former $AuPPh_3$ triangle to one phosphine site of the latter $AuPPh_3$ triangle and vice versa as confirmed by the intense crosspeaks between sites A and sites B in the ^{31}P COSY spectrum of **1** (Figure 2B).

From the doublet nature of sites A and B it can be concluded that the bonding in this cluster is primarily radial; in the case of strong peripheral interactions a triplet pattern for sites A and B would have been observed. The pattern of closely separated peaks for sites A and sites B is most likely not caused by such additional, small peripheral interactions because these peak positions were observed at constant chemical shifts using different field strengths, rather than that a constant peak separation on the frequency scale was observed. At room temperature a broad resonance can be observed near δ −7.0 ppm, in addition to the aforementioned resonances. On lowering the temperature in the interval 273–233 K this signal sharpens to result in two separate singlets at δ −5.0 and −7.8 ppm at 233 K (Figure 3); this behavior is reversible. The relative total intensity of these two singlets equals that of the signal at δ 37.59 ppm, i.e. these former two singlets together correspond to a total of one phosphine. This variable-temperature behavior is explained by a reversible dissociation–addition mechanism of the copper-bonded phosphine (P(8)): The singlet near δ −5.0

$$[Pt(PPh_3)(AuPPh_3)_6(Cu_4Cl_3PPh_3)]^+ \rightleftharpoons [Pt(PPh_3)(AuPPh_3)_6(Cu_4Cl_3)]^+ + PPh_3 \quad (4)$$

1a

ppm originates from the copper-bonded phosphine (P(8)), whereas the singlet near δ −7.8 ppm originates from the free PPh_3; this was indicated by addition of PPh_3. The geometry of **1a** is probably similar to that known for **3**, where the solid-state structure is that without a copper-bonded phosphine (vide

(35) Kappen, T. G. M. M.; Schlebos, P. P. J.; Bour, J. J.; Bosman, W. P.; Smits, J. M. M.; Beurskens, P. T.; Steggerda, J. J. *Inorg. Chem.* **1994**, *33*, 754.
(36) Braunstein, P.; Freyburger, S.; Bars, O. *J. Organomet. Chem.* **1988**, *352*, C29.
(37) Hallam, M. F.; Mingos, D. M. P.; Adatia, T.; McPartlin, M. *J. Chem. Soc., Dalton Trans.* **1988**, 335.
(38) Van Koten, G.; Jastrzebski, J. T. B. H.; Noltes, J. G. *Inorg. Chem.* **1977**, *16*, 1782.
(39) Pathaneni, S. S.; Desiraju, G. R. *J. Chem. Soc., Dalton Trans.* **1993**, 319.
(40) Kanters, R. P. F.; Steggerda, J. J. *J. Cluster Sci.* **1990**, *1*, 229.
(41) Van der Velden, J. W. A.; Bour, J. J.; Bosman, W. P.; Noordik, J. H. *Inorg. Chem.* **1983**, *22*, 1913.
(42) Vollenbroek, F. A.; van der Velden, J. W. A.; Bour, J. J.; Steggerda, J. J. *Inorganic Reactions and Methods*; Zuckerman, J. J., Hagen, A. P., Eds.; VCH Publishers: New York, 1991; Vol. 13, pp 351–354.
(43) Kanters, R. P. F.; Schlebos, P. P. J.; Bour, J. J.; Steggerda, J. J.; Maas, W. E. J. R.; Janssen, R. *Inorg. Chem.* **1991**, *30*, 1709.

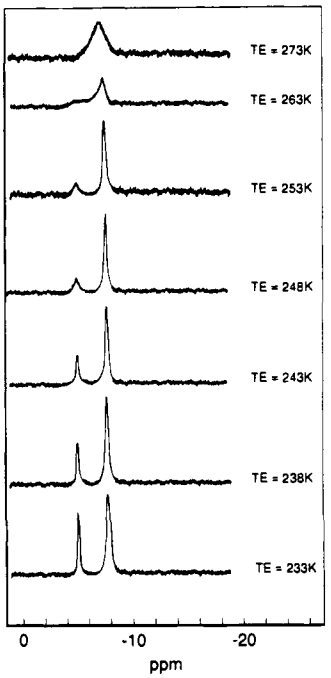

Figure 3. Variable-temperature (273−233 K) ^{31}P NMR spectra (202.462 MHz) of the Cu−PPh_3/PPh_3 region of $[Pt(PPh_3)(AuPPh_3)_6(Cu_4Cl_3PPh_3)](NO_3)$ (**1**).

Table 4. Estimated Equilibrium Constants, K, for the Reaction **1** ⇌ **1a** + PPh_3 at Different Temperatures

T (K)	K (mol·L^{-1})[a]	T (K)	K (mol·L^{-1})[a]
273	0.204	243	0.0516
263	0.166	238	0.0429
253	0.0705	233	0.0239
248	0.0665		

[a] The equilibrium constant K = [**1a**][PPh_3]/[**1**]; concentrations were calculated by means of the integrals of the ^{31}P NMR resonances of the copper-bonded phosphine of **1** and of free PPh_3; the concentration of **1a** equals that of free PPh_3.

infra). It is noteworthy that the resonances of the platinum-bonded and gold-bonded phosphines, as reported above, remain unchanged in this temperature interval. This means that, except for the position and coordination of Cu(1), the cluster geometry of **1a** is almost identical to that of **1**. This corresponds to the aforementioned nonfluxionality: the cluster core is too crowded so (i) no intramolecular phosphine fluxionality is allowed and (ii) only minor reorganizations of the geometry after phosphine dissociation can occur (except for the Cu(1) atom, which might be repositioned closer to the other Cu atoms, resulting in a geometry analogous to what is observed in the solid-state structure of **3**; vide infra). Apparently, these minor reorganizations cause only very small frequency differences between the (gold and platinum) phosphines of **1** and those of **1a** so that the fast-exchange situation is observed for these resonances in the entire temperature interval.

Simulation[44] of the Cu−PPh_3/PPh_3 region of the variable-temperature ^{31}P NMR spectra with respect to line shape roughly showed the forward reaction constant, k_{diss}, for reaction 4 to range from ca. 400 Hz (at 273 K) to less then 20 Hz (at 233 K). Integration[44] of these spectra provided us with the absolute concentrations of **1** and free PPh_3 and therefore also of **1a**. From this the equilibrium constants, K, for reaction 4 at different temperatures could be estimated (see Table 4):

$$K = [\mathbf{1a}][PPh_3]/[\mathbf{1}]\ (\text{mol·L}^{-1})$$

The temperature dependence of this equilibrium constant provides information on the enthalpy and entropy change for the phosphine dissociation of reaction 4: $\Delta H_{diss} \approx +27$ kJ·mol^{-1} and $\Delta S_{diss} \approx +88$ J·mol^{-1}·K^{-1} are estimated from the slope and the intercept of the ln$K$ *vs* $1/T$ plot as $-\Delta H_{diss}/R$ and $\Delta S_{diss}/R$, respectively. These values are in reasonable agreement with those that might be expected for a dissociation like reaction 4;[45] therefore they provide additional support for the correctness of the proposed dissociation−addition mechanism.

The $^{195}Pt\{^1H\}$ NMR spectrum of **1** is observed at δ −5761 ppm with a complex splitting pattern (Figure 4A), due to J couplings to the platinum-bonded and gold-bonded phosphines, that can be simulated with ^1J(Pt−P)(doublet) = 2476 Hz, ^2J(Pt−P)(quartet) = 358 Hz, and ^2J(Pt−P)(quartet) = 450 Hz. Therefore the ^{195}Pt NMR coupling pattern is in agreement with the ^{31}P NMR data and with the geometry of **1** as discussed above.

The ^{195}Pt NMR spectrum without proton decoupling is unchanged with respect to the $^{195}Pt\{^1H\}$ NMR spectrum. This shows that there is no hydride ligand present on **1**.

Fast Atom Bombardment Mass Spectroscopy (FAB-MS). FAB-MS has been shown to be a successful technique for the determination of the correct molecular composition of cationic cluster compounds.[7,35] The positive ion FAB-MS of **1** in the 2600−4000 mass range (Figure 5) has a large number of peaks; a selection of the centroids of heavy fragments as well as their assignments is given in Table 5. The result is in good agreement with the composition and the structure of **1** as discussed above. No peaks with masses higher than that of M^+ are observed. The relative abundance of the peak corresponding to the mass of M^+ is very low, whereas that of $(M - PPh_3)^+$ is more explicit. This might be related to the rather labile coordination of the copper-bonded phosphine as discussed above.

(a) Synthesis and Characterization of $[Pt(PPh_3)(AuPPh_3)_6(Cu_4Br_3(PPh_3)_y)](NO_3)$ (2) (y = 0 or 1). The reaction of $[Pt(AuPPh_3)_8](NO_3)_2$ with $[PPh_3CuBr]_4$ in acetone yields a mixture of compounds in which **2** is present in about 50%; several attempts to isolate **2** from this mixture were not successful. However, comparison of the ^{31}P NMR data of compounds **1**, **2**, and **3** (vide infra), together with a comparison of the routes of synthesis of these three compounds, indicates **2** to be closely related to **1** and **3**. Therefore **2** is most probably formulated as $[Pt(PPh_3)(AuPPh_3)_6(Cu_4Br_3(PPh_3)_y)](NO_3)$ (in which y = 0 or 1). As the crystal structure of **1** shows the presence of a copper-bonded phosphine, which can dissociate reversibly in solution, and **3** shows the absence of such a copper-bonded phosphine it is not clear whether **2** has such a copper-bonded phosphine or not.

(b) Synthesis, Characterization, and Crystal Structure of $[Pt(PPh_3)(AuPPh_3)_6(Cu_4I_3)](NO_3)$ (3). When $[Pt(AuPPh_3)_8](NO_3)_2$ is made to react with $[PPh_3CuI]_4$ in acetone, **3** is obtained. A single crystal of **3** could be obtained and an X-ray analysis of this crystal revealed the solid-state structure of **3**. Cluster **3** was also characterized by ^{31}P NMR spectroscopy and its presence was also confirmed by FAB-MS.

Since the red crystals, obtained by slow diffusion, all had the same morphology it is assumed that the solid consists of a single compound (**3**) of which the crystal structure will be reported below. However, the ^{31}P NMR data show that in solution two rather similar compounds are present (**3** and **X**, vide infra); since we were not able to separate these two

(44) Budzelaar, P. H. M. *geNMR, NMR Simulation Program V3.4*; IvorySoft: Amsterdam, 1992.

(45) Sunick, D. L.; White, P. S.; Schauer, C. K. *Inorg. Chem.* **1993**, *32*, 5665.

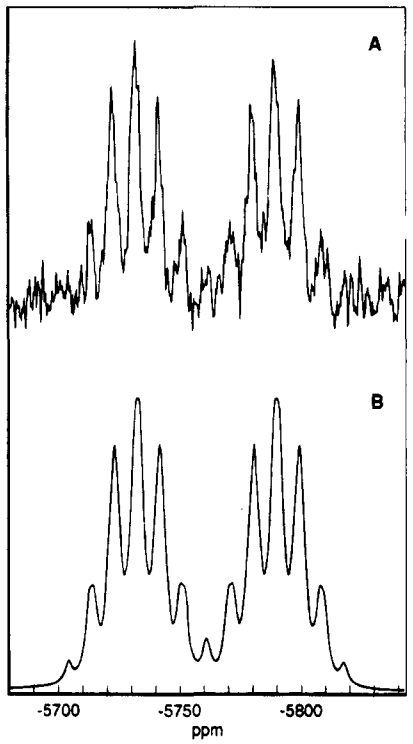

Figure 4. $^{195}Pt\{^1H\}$ NMR spectrum (43.02 MHz) of the cluster compound $[Pt(PPh_3)(AuPPh_3)_6(Cu_4Cl_3PPh_3)](NO_3)$ (**1**): (A) experimental spectrum and (B) simulated spectrum (see Results and Discussion) ($W_{1/2}$ for ^{195}Pt set to 150 Hz).

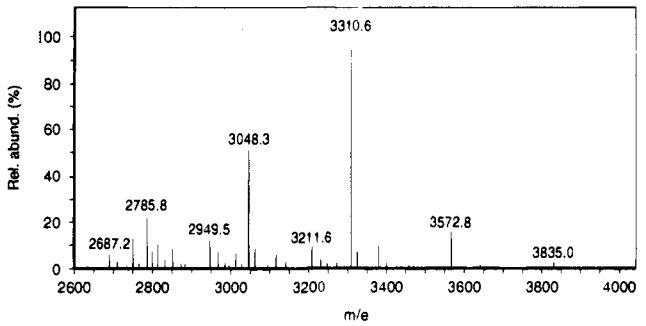

Figure 5. Low-resolution positive ion FAB-MS spectrum of the cluster $[Pt(PPh_3)(AuPPh_3)_6(Cu_4Cl_3PPh_3)](NO_3)$ (**1**) in the *m/e* 2600−4000 mass range.

Table 5. Positive Ion FAB-MS Data for **1** (M^+ = $[Pt(PPh_3)(AuPPh_3)_6(Cu_4Cl_3PPh_3)]^+$)

rel mass, *m/e*			
obsd[a]	calcd	% abundance	assignment
3835.0	3835.75	2	M^+
3572.8	3573.46	16	$(M - PPh_3)^+$
3310.6	3311.17	100	$(M - 2PPh_3)^+$
3211.6	3212.17	9	$(M - 2PPh_3 - Cu - Cl)^+$
3048.3	3048.88	52	$(M - 3PPh_3)^+$
2949.5	2949.88	12	$(M - 3PPh_3 - Cu - Cl)^+$
2785.8	2786.59	23	$(M - 4PPh_3)^+$
2687.2	2687.59	6	$(M - 4PPh_3 - Cu - Cl)^+$

[a] Not matched.

compounds or even to change their ratio, we believe that there is a simple chemical reaction converting **3** and **X**. Although no formulation of **X** can be given yet, we think that **X** most probably contains two $Pt(AuPPh_3)_6$ moieties.

Crystal Structure. The X-ray structure analysis, together with the ^{31}P NMR data (vide infra), shows that the solid-state structure of **3** (Figure 6) is very similar to that of **1** (Figure 1), except for the copper-bonded phosphine which is missing in **3**.

Table 6. ^{31}P NMR Data for **1**, **2**, and **3**

	1	**2**	**3**
$\delta(Au-P)_A$ (ppm)	58.8	58.2	57.0
$^2J(P-^{195}Pt)$ (Hz)	450	460	445
$^4J(P-P)$ (Hz)	66	68	66
$\delta(Au-P)_B$ (ppm)	52.3	51.6	50.7
$^2J(P-^{195}Pt)$ (Hz)	358	344	368
$^4J(P-P)$ (Hz)	66	68	66
$\delta(Pt-P)$ (ppm)	37.6	38.4	36.2
$^1J(P-^{195}Pt)$ (Hz)	2476	2479	2458

Table 7. Positive Ion FAB-MS Data Corresponding to **3** (M^+ = $[Pt(PPh_3)(AuPPh_3)_6(Cu_4I_3)]^+$)

rel mass, *m/e*		%	
obsd[a]	calcd	abundance	assignment
3718.8	3719.37	100	$(M - Cu - I + NO_3)^+$
3585.5	3585.52	36	$(M - PPh_3)^+$
3456.7	3457.08	33	$(M - PPh_3 - Cu - I + NO_3)^+$
3395.1	3395.07	48	$(M - PPh_3 - Cu - I)^+$
3323.5	3323.66	20	$(M - Au - PPh_3 - I + NO_3)^+$
[or:	3323.23	20	$(M - 2PPh_3)^+$]
3260.1	3260.11	13	$(M - Au - PPh_3 - Cu - I + NO_3)^+$
3194.4	3194.79	20	$(M - 2PPh_3 - Cu - I + NO_3)^+$
3132.8	3132.78	52	$(M - 2PPh_3 - Cu - I)^+$

[a] Not matched.

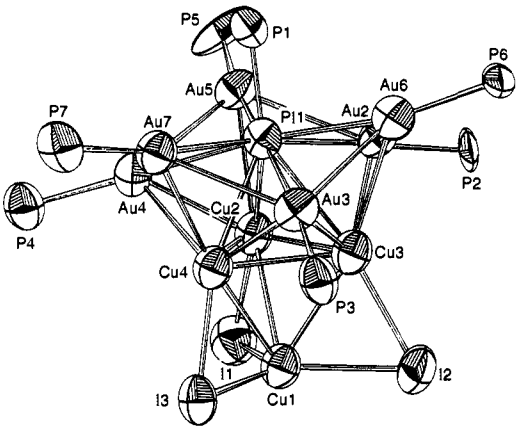

Figure 6. X-ray structure of $[Pt(PPh_3)(AuPPh_3)_6(Cu_4I_3)](NO_3)$ (**3**) with atom labeling for Pt, Au, Cu, P, and Cl. Phenyl rings and the NO_3^- ion have been omitted for the sake of clarity. Thermal ellipsoids are at 50% probability.

The six $AuPPh_3$ units are bonded to the (central) platinum atom in two layers which are arranged in a staggered way; a PPh_3 ligand is coordinated to this platinum atom. The Cu_4I_3 unit consists of an almost ideal regular Cu_4 tetrahedron (Cu−Cu distances: 2.69−2.72 Å), in which three μ_2-I ligands are bridging the copper atoms; this Cu_4 tetrahedron is η^3 (face) bonded to the platinum atom through Cu(2), Cu(3), and Cu(4). However, short copper−gold and copper−platinum distances indicate that these copper atoms are part of the metal core. These three copper atoms, together with the six Au−P units, the Pt−P unit, and the three μ_2 halides, are arranged in a way that only slightly deviates from that in **1** (also see Tables 2 and 3). The only substantial difference between the solid-state structures of **1** (Figure 1) and **3** (Figure 6), apart from the absence of PPh_3 bonded to Cu(1) in **3**, is that in **3** Cu(1) is situated more toward the Cu(2)−Cu(3)−Cu(4) triangle. We think that the large iodide ligands in **3** prevent coordination of a PPh_3 ligand to Cu(1); even the smaller chloride ligands in **1** allow such phosphine coordination only when Cu(1) moves out of its "cuprophilic" pocket (see above). In this vision the solid-state structure of **3** can be regarded as representative of the structure of **1a**; i.e.

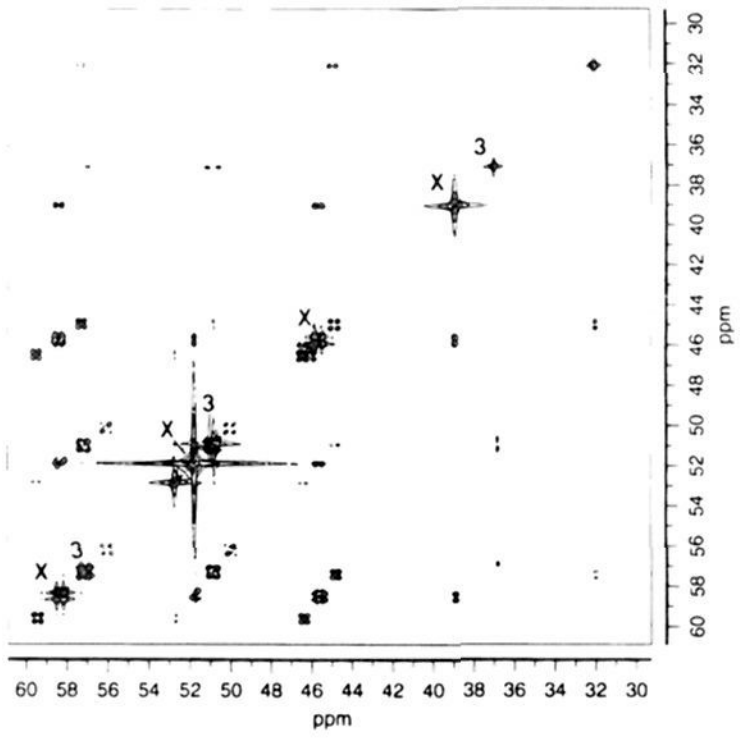

Figure 7. ^{31}P COSY NMR spectrum (202.462 MHz) at 298 K of the mixture containing $[Pt(PPh_3)(AuPPh_3)_6(Cu_4I_3)](NO_3)$ (**3**) and the unknown product **X** (main peaks on the diagonal are labeled for compounds **3** and **X**; other peaks on the diagonal are ^{195}Pt satellites of these main peaks). For coupling patterns compare to Figure 2B and see text.

after phosphine dissociation from **1**, Cu(1) moves toward the Cu(2)−Cu(3)−Cu(4) triangle to result in **1a**.

The large increase of the Cu−Cu(1) distances in going from the solid-state structures of **3** to **1** (Tables 3 and 2) implies that the bridging halides are vital in keeping the Cu_4 unit together.

The central platinum atom of **3**, like that of **1**, is surrounded in a (quasi-)spheroidal symmetry by the $AuPPh_3$ units, the platinum-bonded phosphine, and the Cu_4 unit. This classification is justified by the topological parameters S and P,[40] which amount to 0.97 and 0.99, respectively. This spheroidal surrounding is in agreement with the $(S^{\sigma})^2(P^{\sigma})^6$ electron configuration (18 electrons) of **3**.

NMR Spectroscopy. As for **1** and **2** the ^{31}P NMR spectrum of **3** at room temperature is also indicative of a nonfluxional cluster compound. The platinum-bonded phosphine resonates at δ 36.2 ppm, and the gold-bonded phosphines are observed as two doublets; shoulders on these doublet peaks again indicate that these doublets are a result of closely separated signals. The coupling pattern and its interpretation are identical to those explained for **1** and **2**. This was evidenced by the ^{31}P COSY spectrum of **3** (Figure 7, peaks labeled with "**3**"), which shows a coupling pattern identical to that of **1** (Figure 2B). From this ^{31}P COSY spectrum it could be inferred that only one other (phosphorus-containing) compound (**X**) was present. The ratio of **3** to **X** is always ca. 1:5. Various attempts to separate **3** and **X** were unsuccessful. Some peaks of **3** and **X** are (partially) overlapping in the ^{31}P NMR spectrum, but proper changing of spectrometer frequency, together with crosspeak analysis from the ^{31}P COSY spectrum, provides clear insight in the coupling patterns of **3** and **X** (Figure 7). The coupling pattern of the unknown product **X** is largely similar to that of **1**, **2**, and **3**, but it has an additional intense singlet at δ 51.8 ppm (for full ^{31}P NMR data of the unknown product see the Experimental Section). This intense singlet proves that this signal does not belong to **3**.

Variable-temperature ^{31}P NMR experiments (295−213 K) did not reveal the presence of a copper-bonded phosphine as observed for **1**. This is in agreement with the absence of such a phosphine in the solid-state structure of **3**.

Fast Atom Bombardment Mass Spectroscopy (FAB-MS). A selection of the centroids of the heavy fragments (those being

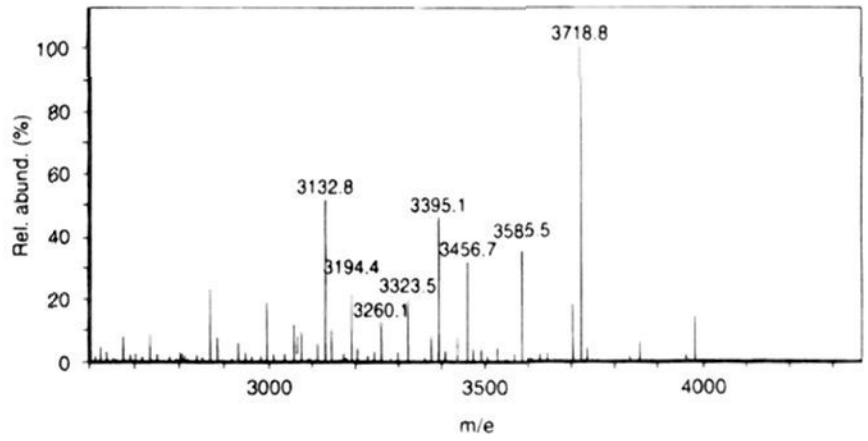

Figure 8. Low-resolution positive ion FAB-MS spectrum of the reaction mixture of $[Pt(AuPPh_3)_8](NO_3)_2$ and $[PPh_3CuI]_4$, containing **3** and **X**. The numbered peaks are in agreement with the composition and structure of **3** (see Results and Discussion).

in agreement with the composition and structure of **3** as discussed above) as well as their assignments is given in Table 7. This FAB-MS shows several peaks where the NO_3 unit is still present in the molecular fragment, this in contrast to what is observed from the FAB-MS of **1**. A tempting explanation for this difference is that in **3** the nitrate is somewhat more attracted to the cluster due to Cu(1), as compared to the situation in solid **1** where Cu(1) is shielded by coordination of a PPh_3.

Peaks with masses higher than M^+ are observed, but due to the possible presence of the unknown product **X** in the sample, or some minor contamination, nothing can be said about these peaks.

In this paper it was shown that the newly prepared compounds are $PtAu_6Cu_4$ clusters that can be regarded as $PtAu_6$ and Cu_4 frames which have been fused together. The Cu_4X_3 moiety is recognizable as the metal halide frame of the parent cubane-like $[PPh_3CuX]_4$ (X = Cl, Br, I). We think this to be a strong indication that the cluster growth has occurred by merging the Cu_4 unit into the $PtAu_8$ frame. The Pt takes the μ_3 position over one of the Cu_3 faces replacing one of the halides, which has dissociated. To release steric strain two $AuPPh_3^+$ together with the copper-bonded phosphines dissociate, whereas the remaining halides take μ_2 positions to reach a stable final product.

This view of cluster merging is additionally supported by reactions of clusters like $[Pt(AuPPh_3)_8](NO_3)_2$ with mononuclear metal compounds like $Ag(PPh_3)(NO_3)$ and CuCl: these reactions yield products in which the Ag or Cu atoms have been added to the cluster framework in non-adjacent positions.[4−6]

Acknowledgment. This investigation was supported by the Netherlands Foundation for Chemical Research (SON) with fundamental support from the Netherlands Organization for the Advancement of Pure Research (NWO). Dr. M. F. J. Schoondergang is thanked for his preliminary studies.[6] We acknowledge Mrs. Véronique J. Zwikker and Mr. Roger A. J. M. Klaver for their contributions. Prof. L. H. Pignolet of the University of Minnesota is gratefully thanked for his fruitful discussions and for providing the opportunity to do FAB-MS experiments.

Supporting Information Available: A listing of crystallographic details and fractional positional parameters, anisotropic thermal parameters, and bond distances and angles (42 pages). This material is contained in many libraries on microfiche, immediately follows this article in the microfilm version of the journal, and can be ordered from the ACS, and can be downloaded from the Internet; see any current masthead page for ordering information and Internet access instructions.

JA942684E